

Novel electronic wave interference patterns in nanographene sheets

This article has been downloaded from IOPscience. Please scroll down to see the full text article.

2002 J. Phys.: Condens. Matter 14 L605

(<http://iopscience.iop.org/0953-8984/14/36/102>)

View [the table of contents for this issue](#), or go to the [journal homepage](#) for more

Download details:

IP Address: 171.66.16.96

The article was downloaded on 18/05/2010 at 12:33

Please note that [terms and conditions apply](#).

LETTER TO THE EDITOR

Novel electronic wave interference patterns in nanographene sheets

Kikuo Harigaya^{1,2,3,4,5}, Yousuke Kobayashi³, Kazuyuki Takai³,
Jérôme Ravier³ and Toshiaki Enoki³

¹ Nanotechnology Research Institute, AIST, Tsukuba 305-8568, Japan

² Synthetic Nano-Function Materials Project, AIST, Tsukuba 305-8568, Japan

³ Tokyo Institute of Technology, Oh-okayama, Meguro-ku 152-8551, Japan

E-mail: k.harigaya@aist.go.jp

Received 18 July 2002

Published 29 August 2002

Online at stacks.iop.org/JPhysCM/14/L605

Abstract

Superperiodic patterns extending over a large distance in a nanographene sheet observed using a scanning tunnelling microscope are discussed in terms of the interference of electronic wavefunctions. The period and the amplitude of the oscillations decrease spatially in one direction. We explain the superperiodic patterns with a static linear potential, theoretically. In the $k \cdot p$ model, the oscillation period decreases, and agrees with experiments. The spatial difference of the static potential is estimated as 1.3 eV for 200 nm in distance, and this value seems to be reasonable preserving for the potential difference under the action of perturbations, for example, phonon fluctuations and impurity scatterings. It turns out that the long-distance oscillations arise from the band structure of the two-dimensional graphene sheet.

1. Introduction

Nanographene sheets are attractive materials, because their magnetic and transport properties show novel and peculiar properties, originating from nonbonding states localized at the zigzag edges [1, 2]. Theoretical works [2–5] have been performed to clarify the mechanisms of the unique magnetism. It has been found that the A–B stacking and the presence of the localized electronic spins originating from the open-shell nature are favourable conditions for the magnetism.

On the other hand, direct observation using a scanning tunnelling microscope (STM) is a powerful method for structural analysis (for example, the presence of a single nanographene sheet has been observed using a STM [6]) as well as for investigation of electronic properties.

⁴ Author to whom any correspondence should be addressed.

⁵ <http://staff.aist.go.jp/k.harigaya/>

The interlayer distance of a single nanographene sheet on a highly oriented pyrolytic graphite (HOPG) substrate has been found to be about 0.35–0.37 nm and this is larger than that for bulk material [6]. In a recent study, we have found superperiodic patterns with extremely long periodicity in STM images of a nanographene sheet which varies spatially [7]. In this letter, we give an explanation for this novel result in terms of the interference of electronic wavefunctions.

In order to understand the origins of the long-distance oscillations which were observed, we will make a comparison with the theoretical electron densities using the model of a free electron confined within an infinite square well, and also using the $k \cdot p$ model [8, 9] for the two-dimensional graphene sheet. One of the present authors has used the model to explain the multi-channel Kondo effect [10] and the Cooper pair propagation [11] in metallic carbon nanotubes. In the graphene sheets, superperiodic patterns in STM images due to the Moiré origins for the A–B stacking [12] and structural deformations [13] have been reported in the literature. However, the observed superperiodic patterns with quite long periods over 10 nm seem not to arise from the Moiré mechanism, and our finding calls for new interpretations. We assume the presence of a static potential with a linear decrease in one direction. The calculated local electron density will be compared with the experiments. We will clarify that the long-distance oscillations are due to the presence of electrons with the band structure of a two-dimensional graphene sheet.

This letter is organized as follows. In section 2, the experimental results are briefly reviewed. In section 3, calculations using the free electron model are compared with experiments. In section 4, the analysis with the $k \cdot p$ model is performed. The letter is closed with a summary in section 5.

2. STM observations

In this section, the experimental data are briefly reviewed. In figure 1, an STM image of the graphene sheet with a necktie shape is shown. The detail will be published elsewhere. The distance between the graphene necktie and the substrate is over 0.8 nm, suggesting that it consists of a stacking of two graphene layers, which interact weakly with the HOPG substrate. Interestingly, the period and the amplitude of the oscillations decrease from the top to the bottom along the graphene necktie. The oscillation period is one order of magnitude larger than that of the Moiré pattern due to stacking [12], and therefore this possibility can be excluded. We can assume effects of long-distance periodic structural deformations [13] in the graphene surface or interference effects of electronic wavefunctions.

We have also observed that the oscillation period becomes longer on placing a nanographene flake on the graphene necktie, as shown in figure 2. The size of the flake is about 10 nm in width and 100 nm in length. Similar sizes of the nanographene flakes have been assumed in the model calculations [4]. The oscillation period seems to be doubled in the upper region of the necktie after addition of one flake. The oscillation below the flake seems to be only slightly modified by the flake. Such an effect on the oscillations cannot be explained by some structural modulations. Therefore, the oscillation patterns could be the effect of interference of the electronic wavefunctions in the graphene surface.

3. Free electron model

We will characterize the interference patterns theoretically. The two-dimensional coordinate is defined such that the y -axis is along the long direction of the graphene necktie. The x -

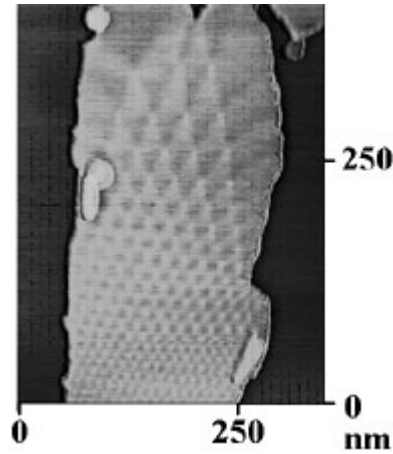


Figure 1. A STM image of the superperiodic pattern on a necktie-shaped graphene plate on a HOPG substrate. The observation at room temperature and under atmospheric pressure was carried out under the following conditions: the bias voltage $V = 200$ mV and the current $I = 0.7$ nA.

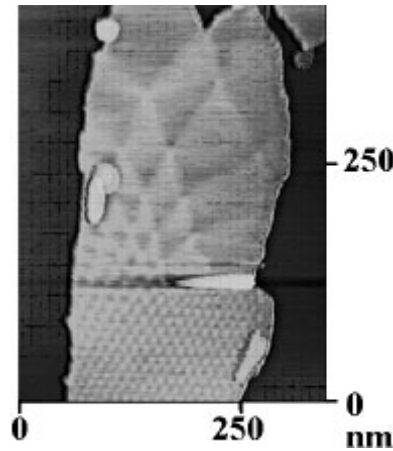


Figure 2. A STM image of the superperiodic pattern on the necktie-shaped graphene sheet observed in figure 1 after a nanographene flake is placed on it.

axis is perpendicular to the y -axis. By assuming an electric static potential $-Fy$ which is proportional to the y -axis coordinate, and a confinement effect due to the well-shaped potential within $-d/2 < x < d/2$, we obtain the Schrödinger equation:

$$\left[-\frac{\hbar^2}{2m} \left(\frac{\partial^2}{\partial x^2} + \frac{\partial^2}{\partial y^2} \right) + V_{\text{well}}(x) - Fy \right] \psi(x, y) = E \psi(x, y), \quad (1)$$

where $V_{\text{well}}(x)$ is a well potential with infinite depth. The electron density with the energy E is written as

$$|\psi(x, y)|^2 = \sum_n a_n |\psi_x(E_n) \psi_y(E - E_n)|^2, \quad (2)$$

where a_n is the coefficient of occupancy with the quantum number n , $\psi_x(E_n)$ is the solution in the well in the x -direction, and $\psi_y(E - E_n)$ is the solution for the potential term $-Fy$. The

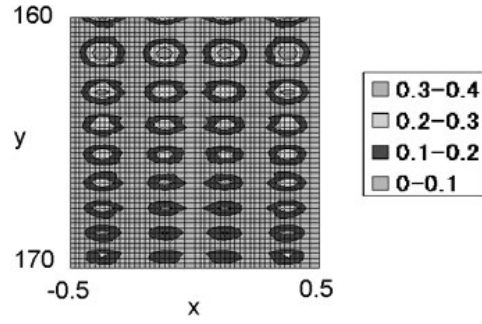


Figure 3. A two-dimensional plot of the electron density calculated using the free electron model. The bottom and left axes are shown in arbitrary units. The quantum number $n = 4$ is taken for the standing wave within the infinite well; $-0.5 < x < 0.5$ with $d = 1$.

solution in the well is

$$\psi_x(E_n) = \begin{cases} A \cos\left(\frac{n\pi x}{d}\right) & \text{for odd } n \\ A \sin\left(\frac{n\pi x}{d}\right) & \text{for even } n, \end{cases} \quad (3)$$

with $E_n = \pi^2 \hbar^2 n^2 / 2md^2$ and $A = \sqrt{2/d}$. The solution for the linear potential is

$$\psi_y(E - E_n) = \Phi\left[-\left(\frac{2mF}{\hbar^2}\right)^{1/3} \left(x + \frac{E}{F} - \frac{E_n}{F}\right)\right], \quad (4)$$

where $\Phi(x)$ is the Airy function

$$\Phi(x) = \frac{1}{\sqrt{\pi}} \int_0^\infty \cos\left(\frac{u^3}{3} + ux\right) du. \quad (5)$$

The local density of states of electrons with $a_n = 1$ only for $n = 4$ is shown in figure 3. We can explain the decrease of the oscillation period and the amplitude along the y -direction theoretically. This property arises from the form of the Airy function. As the coordinate y becomes larger, the potential becomes deeper. This results in increase of the effective kinetic energy, and thus the wavenumber of the oscillation becomes larger. There is a standing wave in the x -direction. However, we cannot explain the details of oscillations in the x -direction of figure 1; possibly they are caused by the effects of the complex shape of the boundary in the graphene necktie.

Even though the oscillation in the well is uniform spatially, we can compare the oscillation patterns in the y -direction at least. Figure 4 shows a comparison with the experiment where the peak positions along the long axis of the necktie are plotted. The decrease of the amplitude of the theoretical curve seems more rapid than that of the experimental data. The strength of the static potential is $F = 5.26 \times 10^{-6} \text{ eV nm}^{-1}$, using the free electron mass. The potential variation over the distance 200 nm is $1.1 \times 10^{-3} \text{ eV}$, and this is quite small. Phonon fluctuation effects or the presence of impurities can override such a small potential change. This difficulty might be due to the assumption of the free electron model of this section. The exact solution using the Airy function for the Schrödinger equation with a linear potential is known from textbooks on quantum mechanics [14], and the comparison with this simple textbook result has been our main interest in this section.

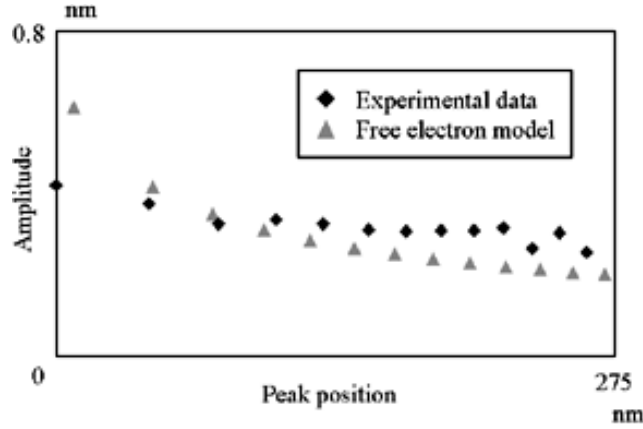


Figure 4. Comparison of the electron wave patterns found from the STM and the free electron theory. Experimental peak positions along the perpendicular direction of figure 1 are plotted as diamonds. The results of the fitting by the one-dimensional free electron model are shown by triangles.

4. Continuum $k \cdot p$ model

In order to substantiate the analysis of the interference patterns, we give a comparison with the calculation of the model for the graphene plane. Here, we use the continuum $k \cdot p$ model [8, 9]. The Hamiltonian around the K -point with the linear potential $-Fy$ is

$$H = \begin{pmatrix} -Fy & -i\gamma \frac{\partial}{\partial x} - \gamma \frac{\partial}{\partial y} \\ -i\gamma \frac{\partial}{\partial x} + \gamma \frac{\partial}{\partial y} & -Fy \end{pmatrix}, \quad (6)$$

where $\gamma \equiv (\sqrt{3}/2)a\gamma_0$, a is the bond length, and γ_0 is the hopping integral for neighbouring carbon atoms. This model is solved and the infinite-well potential $V_{\text{well}}(x)$ as used in the previous section is used. The Schrödinger equation $H\Psi = E\Psi$ gives an oscillating solution:

$$\Psi = 2A \begin{pmatrix} \sin\left(\frac{E_n x}{\gamma}\right) \sin\left[\frac{1}{\gamma}\left(\tilde{E}y + \frac{1}{2}Fy^2\right)\right] \\ -i \cos\left(\frac{E_n x}{\gamma}\right) \cos\left[\frac{1}{\gamma}\left(\tilde{E}y + \frac{1}{2}Fy^2\right)\right] \end{pmatrix}, \quad (7)$$

where $E_n = n\pi\gamma/d$ and $\tilde{E} = E - E_n$. The electron density at the A-sublattice point is calculated as

$$|\psi_A(\mathbf{R}_A)|^2 = 4A^2 \sin^2\left(\frac{n\pi x}{d}\right) \left\{ 1 + \cos[(\mathbf{K} - \mathbf{K}') \cdot \mathbf{R}_A] \sin\left[\frac{2}{\gamma}\left(\tilde{E}y + \frac{1}{2}Fy^2\right)\right] \right\} \quad (8)$$

where \mathbf{R}_A is the lattice point of the A sublattice, \mathbf{K} and \mathbf{K}' are the K - and K' -points in the wavenumber space. We pay particular attention to the long-period oscillating component:

$$\sin^2\left(\frac{n\pi x}{d}\right) \left[\text{constant} + \sin\left(\frac{Fy^2}{\gamma} - \frac{2n\pi}{d}y\right) \right], \quad (9)$$

where we take $E = 0$ at the Fermi energy. This functional form for the quantum number $n = 4$ is plotted in figure 5 with the assumption $d = 1$. The amplitude is spatially constant, and the oscillation period becomes smaller as y becomes larger. We can explain the decrease of the oscillation period found in the experiments of figure 1, although a uniform array for the standing wave would be the result of the simplified theory and this is in contrast with the observations.

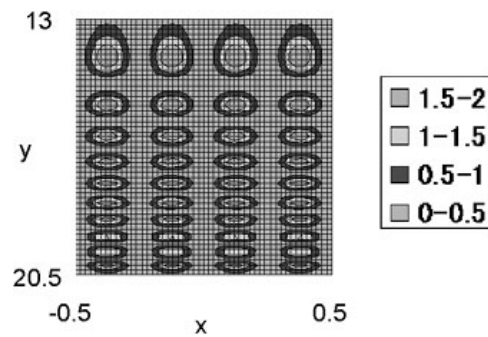


Figure 5. A two-dimensional plot of the electron density calculated using the $k \cdot p$ model. The bottom and left axes are shown in arbitrary units. The quantum number $n = 4$ is taken for the standing wave within the infinite well; $-0.5 < x < 0.5$ with $d = 1$.

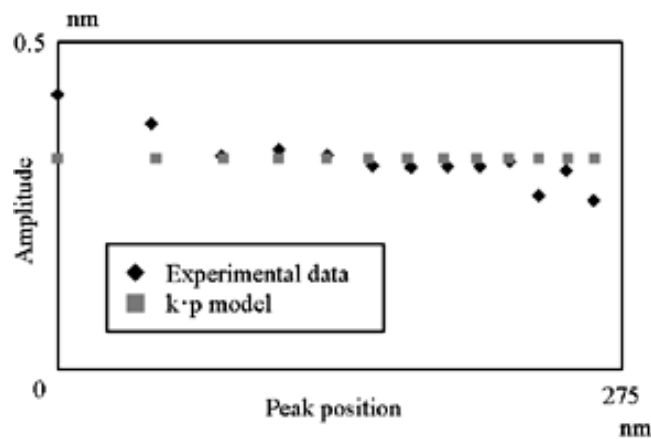


Figure 6. Comparison of the electron wave patterns from the STM and the $k \cdot p$ model. Experimental peak positions along the perpendicular direction of figure 1 are plotted as diamonds. The results of the fitting by the long-distance envelope functional form derived from the $k \cdot p$ model are shown by squares.

The peak positions of the electron density in the long direction of the graphene necktie of figure 1 are plotted in figure 6, and a comparison with the result of equation (9) is given. The slight decrease found in the experiments cannot be reproduced by the result from the $k \cdot p$ model. However, the decrease of the oscillation period agrees fairly well with the experiments. The fitting gives a parameter of the potential gradient of $F = 6.49 \times 10^{-3} \text{ eV nm}^{-1}$. The total potential variation over the distance 200 nm becomes 1.3 eV. Such a magnitude of the potential change would survive thermal lattice fluctuations and can really exist in experiments. The present result by no means implies that the wavefunctions observed with superperiodic amplitudes are those of the electrons which have the energy levels of the graphene plane.

5. Summary

Superperiodic patterns in a nanographene sheet observed using a STM can be explained with two models of electronic wavefunctions in terms of the interference. First, the experimental results have been briefly introduced. The period and the amplitude of the oscillations decrease

spatially in one direction—along the long direction of the graphene necktie. The patterns are superperiodic, and the period is one order of magnitude longer than that of the well-known Moiré pattern observed in A–B stacked graphite systems. This is a novel finding in our experiments.

Next, theoretical characterizations have been reported. We have explained the interference patterns with the static linear potential by using a free electron model and also by using the continuum $k \cdot p$ model. In the free electron model, we have derived the decrease of the oscillation period and the amplitude along the decreasing direction of the linear potential. However, the strength of the linear potential turned out to be unrealistically small. In the $k \cdot p$ case, the oscillation period decreases, and the amplitude is constant. The spatial difference of the static potential is estimated as 1.3 eV for the distance 200 nm, and this value seems to be reasonable for preserving the potential difference under the action of perturbations, for example, phonon fluctuations and impurity scatterings. It turned out that the long-distance oscillations arose from electrons with the band structures of the two-dimensional graphene sheet.

Helpful discussion with Mr M Murata and Professor M Eto, Department of Physics, Keio University, is acknowledged. Useful discussion with members of the Nanomaterials Theory Group, Nanotechnology Research Institute (<http://unit.aist.go.jp/nanotech/>), AIST, and the Enoki-Fukui Laboratory, Department of Chemistry, Tokyo Institute of Technology, is acknowledged, too. This work was partly supported by NEDO under the Nanotechnology Materials Programme (<http://www.nedo.go.jp/kiban/nano/>), and also partly by a Grant-in-Aid for ‘Research for the Future Programme’, Nano-carbons.

References

- [1] Shibayama Y, Sato H, Enoki T and Endo M 2000 *Phys. Rev. Lett.* **84** 1744
- [2] Harigaya K and Enoki T 2002 *Chem. Phys. Lett.* **351** 128
- [3] Harigaya K, Kawatsu N and Enoki T 2001 *Nanonetwork Materials: Fullerenes, Nanotubes, and Related Systems* (New York: American Institute of Physics) pp 529–32
- [4] Harigaya K 2001 *J. Phys.: Condens. Matter* **13** 1295
- [5] Harigaya K 2001 *Chem. Phys. Lett.* **340** 123
- [6] Affoune A M, Prasad B L V, Sato H, Enoki T, Kaburagi Y and Hishiyama Y 2001 *Chem. Phys. Lett.* **348** 17
- [7] Kobayashi Y, Takai K, Ravier J, Enoki T and Harigaya K, 2002 *Master thesis* unpublished results
- [8] Ajiki H and Ando T 1993 *J. Phys. Soc. Japan* **62** 1255
- [9] Ando T and Nakanishi T 1998 *J. Phys. Soc. Japan* **67** 1704
- [10] Harigaya K 2000 *New J. Phys.* **2** 9
- [11] Harigaya K 2000 *J. Phys.: Condens. Matter* **12** 7069
- [12] Kobayashi K 1996 *Phys. Rev. B* **53** 11 091
- [13] Bernhardt T M, Kaiser B and Rademann K 1998 *Surf. Sci.* **408** 86
- [14] Landau L D and Lifshitz E M 1977 *Quantum Mechanics (Non-Relativistic Theory)* (Oxford: Pergamon) appendix